Effects of Chemical Pressure on Rare-Earth Oxide GdNIn0.7Co0.3O3 with Nonmagnetic Element Substitution

Chemical Pressure Effects of Non-Magnetic Element Substitution on Rare Earth Oxide $GdMn_{0.7}Co_{0.3}O_3$

JianHua Bao, Shunsuke Ohsugi, Hiroki Kunita, Yusuke Amakai, Naoki Momono,

and Hideaki Takano

Graduate School of Engineering, Muroran Institute of Technology,
27-1 Mitsumoto-cho, Muroran, Hokkaido 050-8585, Japan

Chemical pressure effects were studied for $Gd_{1-y}R_yMn_{0.7}Co_{0.3}O_3$ (R= non-magnetic rare-earth element) with y = 0.1, 0.3 and 0.5. Substitution of Gd with La, Y or Lu in orthorhombic $Gd_{1-y}R_yMn_{1-x}Co_xO_3$ induced a systematic unit-cell volume change. Our results reveal that increasing or decreasing the average ionic radius of the rare-earth elements in the compounds affects the magnetic ordering temperature T_C. The reduction in the proportion of Gd due to substitution by non-magnetic elements weakens the spin reversal effect.

1. Introduction

ABO_3-type perovskites with the formula $RMnO_3$ (R: rare-earth element) have been investigated extensively as multiferroic materials.[1-14] When Mn is replaced with other 3d transition metal elements, the magnetic and electrical properties are closely related to the Mn^{3+}/Mn^{4+} ratio, but other factors may also influence the magnitude and nature of the magnetic interactions. For instance, the ionic size of A site or B site cations may affect some geometrical parameters (i.e., the unit-cell volume, the B-O-B bond angle, or the tolerance factor).[8-14] Previous studies on the structural and magnetic properties of $GdMn_{1-x}Co_xO_3$,[13,14] which is orthorhombic for $0 \leq x \leq 1.0$, have shown that substitution of Mn with other transition metal elements such as Co, Ni, and Cu causes a transformation of Mn^{3+} to Mn^{4+}. For $x \geq 0.25$, at the canted magnetic ordering temperature T_C, the field-cooled magnetization (M_{FC}) shows a rapid increase, which results from canting of the Mn and Co moments. In particular, for x=0.3, M_{FC} shows a maximum value at about 40 K, and then decreases rapidly with decreasing temperature and shows a negative magnetization value below the compensation temperature $\underline{T_{comp}}$~20 K.[14] This spin reversal phenomenon can be explained by the antiferromagnetic orientation of the Gd spin relative to the Mn and Co moments.[14,15]

In this work, a systematic study of $Gd_{1-y}R_yMn_{0.7}Co_{0.3}O_3$ with R=La, Y, and Lu is presented, using a solid-state reaction under ambient pressure as the synthesis method. Moreover, the effect of chemical pressure on the structure and magnetic properties is discussed.

2. Experimental Procedure

The samples were prepared by a solid-state reaction method at ambient pressure. High-purity (99.9%) powders of Gd_2O_3, La_2O_3, Y_2O_3, Lu_2O_3, Mn_2O_3, and Co_3O_4 were weighed in appropriate proportions to obtain the desired nominal compositions of $Gd_{1-y}R_yMn_{0.7}Co_{0.3}O_3$. The mixtures were calcined twice. The first sintering process was performed by heating from room temperature to 1150 °C in 8 h, holding for 4 h, and then cooling to room temperature. The second calcining temperature was 1350 °C with a holding time of 8 h; the final sample was obtained after cooling. The samples were characterized by X-ray powder diffraction (XRD) using a diffractometer

(MiniFlex300, Rigaku) with Cu K_α radiation and a Ni K_β filter. The structural parameters were obtained from Rietveld refinement of the XRD data using the RIETAN-FP program.[16] The M_{FC} measurements were performed with a SQUID magnetometer (MPMS, Quantum Design).

3. Result and discussion

3.1 Structure

Figures 1(a), 1(b), and 1(c) show XRD patterns for $Gd_{1-y}R_yMn_{0.7}Co_{0.3}O_3$ with substitution by the non- magnetic elements La, Y and Lu, respectively. These are referred to as the La, Y and Lu series, respectively, hereafter. There were no detected impurity phases, and the patterns indicated that all samples were single-phase with a Perovskite-type orthorhombic structure (space group: *Pnma*). The lattice parameters *a*, *b*, *c* and the unit-cell volume *V* are indicated in Table I. In the La substitution system, *b* and *c* increase greatly with substitution, reflecting the fact that the unit-cell volume *V* greatly increases, and the increase ratio is about 3% when the substitution amount *y* increases from 0.0 to 0.5. On the other hand, *b* and *c* decrease in the Y and Lu substitution systems, and *V* decreases by about 1.3% in Y substitution systems and by about 2.5% in Lu substitution systems. These changes are considered to be due to the differences in the ionic radii of La, Y, and Lu with respect to Gd. Figures 2(a) and 2(b) show *a*, $b(b/\sqrt{2})$, *c*, and *V*, respectively, as a function of the average ion radius $\langle r_A \rangle = (1-y)\, r_{Gd} + y r_R$ (La^{3+}= 1.216Å, Gd^{3+}= 1.107Å, Lu^{3+}= 1.032Å, Y^{3+} = 1.075Å). The parameters *a*, $b(b/\sqrt{2})$, and *c* change as a function of $\langle r_A \rangle$, and appear to become closer to each other with increasing $\langle r_A \rangle$. This indicates that $Gd_{1-y}R_yMn_{0.7}Co_{0.3}O_3$ approaches the cubic perovskite structure with increasing $\langle r_A \rangle$. On the other hand, it seems that *V* is linearly related to $\langle r_A \rangle$, and is independent of the substituted ions. This volume change represents the chemical pressure effect.

3.2 Magnetic properties

In Fig. 3, we show the temperature dependence of M_{FC}. It shows a rapid increase at T_C with decreasing temperature, which results from canting of the Mn and Co moments. T_C increases rapidly

with increasing concentration y for the La series, decreases with increasing y for the Y series, and decreases rapidly with increasing y for the Lu series. These changes in T_C correspond to the increase and decrease of the unit-cell volume V as shown in Fig. 4, where both V and T_C increase almost linearly as $\langle r_A \rangle$ increases.

The inverse magnetic susceptibility $\chi_{FC}^{-1}=H/M_{FC}$, shown in Figs. 5(a), 5(b), and 5(c) for the La series, Y series, and Lu series, respectively, can be fitted above about 200 K using the Curie-Weiss law:

$$\boldsymbol{\chi} = \frac{M_{FC}}{H} = \frac{C}{T-\Theta} \qquad (1)$$

where C is the Curie constant, and Θ is the Weiss temperature. We can obtain the effective number of Bohr magnetons via

$$P_{\text{eff}} = \sqrt{\frac{3Ck_B}{N\mu_B^2}} \qquad (2)$$

where N is the number of $Gd_{1-y}R_yMn_{0.7}Co_{0.3}O_3$ formula units per gram, k_B is the Boltzmann constant, and μ_B is the Bohr magneton. In Fig. 6, we plot P_{eff} as a function of the R concentration y. Assuming that the electronic states of the ions in the samples are Gd^{3+}(S=7/2), Mn^{4+}(S=3/2), Mn^{3+}(S=2, high spin [HS]), and Co^{2+}(S=3/2, HS), and there is no change in valence on substituting for Gd, the effective number of Bohr magnetons P_{cal} is estimated by the following equation:

$$\boldsymbol{P_{\text{cal}}} = \sqrt{(1-y)P_{Gd^{3+}}^2 + 0.4P_{Mn^{4+}}^2 + 0.3P_{Mn^{3+}}^2 + 0.3P_{Co^{2+}}^2} \qquad (3)$$

where $P_{Gd^{3+}}$, $P_{Mn^{4+}}$, $P_{Mn^{3+}}$, and $P_{Co^{2+}}$ are 7.94, 3.87, 4.90, and 3.87, respectively. P_{eff} and P_{cal} are indicated by colored symbols and a broken line in Fig. 6, respectively. P_{eff} almost corresponds to P_{cal} in spite of the elemental substitution. We then considered that the substitution of Gd by nonmagnetic elements in this system changes the strength of the interaction between Mn and Co without changing the valence of Mn and Co.

In order to explain the decrease in M_{FC} below about 40 K, the so-called spin reversal phenomenon, we adopt the two-sublattice model used in studies of other rare-earth oxides.[8,15,17] In

$$\boldsymbol{M} = \boldsymbol{M_{Mn,\,Co}} + \frac{(1-y)C_{Gd}(H_{int}+H_{ext})}{T-\Theta} \qquad (4)$$

this model, the temperature dependence of M_{FC} can be fitted using the following equation:

where $M_{Mn,\,Co}$ is the saturated moment of the Mn and Co, C_{Gd} is the Curie constant for Gd^{3+}, H_{int} is the internal field at Gd sites due to the canted Mn and Co moments, H_{ext} is the applied field, and Θ is the Weiss temperature. The fitting parameters are listed in Table II. The fitting results for y=0.0 and the La series are shown by a solid line in Fig. 3. We assume that the decrease in magnetization is caused by the interaction of the two magnetic sublattices "Gd" and "Mn and Co", and that the Gd moment is paramagnetic. It is clear that the negative internal field induced by the Mn and Co sublattice affects the Gd sublattice, because at low temperatures the Gd^{3+} spin is oriented in a direction opposite to H_{ext} by H_{int}. With increasing concentration of R elements, $M_{Mn,\,Co}$ increases in the La series, decreases in the Y and Lu series, and shows a more remarkable decrease in the Lu series. H_{int} shows a tendency to decrease with increasing concentration of R elements in all series.

The changes in $M_{Mn,Co}$ indicate that the interaction between Mn and Co is enhanced by increasing V and suppressed by decreasing V. From Table II, we can deduce that the increase in H_{int} is caused by enhancement of the interaction between Mn and Co due to the increase in the maximum value of magnetization in the La series, and also that suppression of the spin reversal is caused by reduction of the Gd content due to substitution by non-magnetic elements.

4. Conclusion

The unit-cell volume V for $Gd_{1-y}R_yMn_{0.7}Co_{0.3}O_3$ increases or decreases depending on the average ion radius $\langle r_A \rangle$, which is dependent on the radius of the substituent R. The change in V due to the substitution by R indicates that this substitution induces a chemical pressure on the crystal structure. Both V and T_C vary linearly with $\langle r_A \rangle$, as shown in Fig. 4. When V increases, it leads to an increase in T_C, due to negative chemical pressure. For positive chemical pressure, decreasing V leads to a decrease in T_C.

On the other hand, the interaction between Mn and Co is enhanced by increasing V and

suppressed by decreasing V, and the enhancement of the interaction increases the maximum value of the magnetization. The substitution of Gd with non-magnetic rare-earth elements changes the unit-cell volume V, an increase in V raises the transition temperature T_C, and a decrease in V lowers T_C. It is considered that these chemical pressure effects and the spin reversal phenomenon occur simultaneously and produce the temperature dependence of M_{FC} shown in Fig. 3.

References

1) T. Kimura, T. Goto, H. Shintani, K. Ishizuka, T. Arima, and Y. Tokura, Nature **426**, 55 (2003).
2) T. Goto, T. Kimura, G. Lawcs, A.P. Ramircz, and Y. Tokura, Phys. Re. Lett. **92**, 257201 (2004).
3) J. Barier, D. Meier, K. Berggold, J. Hemberger, A. Balbashov, J.A. Mydosh, and T. Lorenz, Phys. Rev. **B 73**, 100402(R) (2006).
4) J.R. Sahu, A. Ghosh, A. Sundaresan, and C.N.R. Rao, Mater. Res. Bull. **44**, 2123 (2009).
5) N.A. Spaldin and M. Fiebig Science, **309**, 391 (2005).
6) W.S. Ferreira, J. Agostinho Moreira, A. Almeida, M.R. Chaves, J.P. Araujo, J.B. Oliveira, J.M. Machado Da Silva, M.A. Sa, T.M. Mendonca, P. Simeao Carvalho, J. Kreisel, J.L. Ribeiro, L.G. Vieira, P.B. Tavares, and S. Mendonca Phys. Rev. **B 79**, 054303 (2009).
7) Chuanlong Lin, Yufeng Zhang, Jing Liu, Xiaodong Li, Yanchun Li, Linyun Tang and Lun Xiong, J. Phys: Condensed Matter **24**, 335402 (2012)
8) J. Hemberger, S. Lobina, H.-A. Krug von Nidda, N. Tristan, V.Yu. Ivanov, A.A. Mukhin, A. M. Balbashov, and A. Loidl, Phys. Rev. **B 70**, 024414 (2004).
9) J. Hemberger, F. Schrettle, A. Pimenov, P. Lunkenheimer, V. Yu. Ivanov, A. A. Mukhin, A. M. Balbashov, and A. Loidl1, Phys. Rev. **B 75**, 035118 (2007).
10) D. O'Flynn, C.V. Tomy, M.R. Lees, A. Daoud-Aladine, and G. Balakrishnan, Phys. Rev. **B 83**, 174426 (2010).
11) K. Asai, K. Fujiyoshi, N. Nishimori, Y. Satoh, Y. Kobayashi, and M. Mizoguchi, J. Phys. Soc. Jpn. **67**, 4218 (1998).
12) V.L. Joseph Joly, P.A. Joy, and S.K. Date, Solid State Commun. **121**, 219 (2002).
13) M. M. Farhoudi and X. L. Wang. IEEE Trans. Magn.,**41**, 3493 (2005)
14) O. Peña, A.B. Antunes, G. Martínez, V. Gil, and C. Moure, J. Magn. Magn. Mater. **310**, 159 (2007).
15) A H Cooke, D M Martin and M R Wells, J. Phys. C: Solid State Phys. **7**, 3133 (1974).
16) F. Izumi and K. Momma, Solid State Phenom. **130**, 15-20 (2007).

17) Y. Sakatsume, J. H. Bao, S. Ohsugi, Y. Amakai, and H. Takano, J. Phys. Soc. Jpn. **87**, 124704 (2018).

Figure Captions

Table I Lattice parameters for the solid solutions $Gd_{1-y}R_yMn_{0.7}Co_{0.3}O_3$ (R= La, Y and Lu) as function of y=0.1, 0.3 and 0.5. The upper, middle, and lower values of each parameter correspond to the La, Y, and Lu series, respectively.

Table II Fitting parameters for $Gd_{1-y}R_yMn_{0.7}Co_{0.3}O_3$.

Fig. 1. XRD patterns for $Gd_{1-y}R_yMn_{0.7}Co_{0.3}O_3$ with y=0.1, 0.3 and 0.5 with substitution by the non-magnetic elements La, Y and Lu. (a), (b), and (c) correspond to $Gd_{1-y}La_yMn_{0.7}Co_{0.3}O_3$, $Gd_{1-y}Y_yMn_{0.7}Co_{0.3}O_3$, and $Gd_{1-y}Lu_yMn_{0.7}Co_{0.3}O_3$, respectively,

Fig. 2. Average ion radius $<r_A>$ dependence of (a) lattice parameters a, $b/\sqrt{2}$, and c. and (b) unit-cell volume V.

Fig. 3. Temperature dependence of M_{FC} for $Gd_{1-y}R_yMn_{0.7}Co_{0.3}O_3$. Broken line shows T_C for $GdMn_{0.7}Co_{0.3}O_3$. The solid lines in La series are fits using Eq. (4).

Fig. 4. V and T_C as a function of $<r_A>$. Their linear dependence with the same slope suggests that there is a correlation between V and T_C. The dotted line denotes the ion radius of Gd^{3+}.

Figs. 5. Inverse magnetic susceptibility $\chi_{FC}^{-1}=H/M_{FC}$ for (a) La series, (b) Y series, and (c) for Lu series.

Fig. 6. R concentration dependence of effective magnetic moment P_{eff} for $Gd_{1-y}R_yMn_{0.7}Co_{0.3}O_3$ (R=La, Y, and Lu).

Table I

Lattice parameters of the solid solutions $Gd_{1-y}R_yMn_{0.7}Co_{0.3}O_3$ (R= La, Y and Lu) as function of y=0.1, 0.3 and 0.5. The upper, middle, and lower values of each parameter correspond to the La, Y, and Lu series, respectively.

***y*(La)** ***y*(Y)** ***y*(Lu)**	**0.0**	**0.1**	**0.3**	**0.5**
		5.6301	5.6018	5.5724
***a*/Å**	5.6425	5.6429	5.6419	5.6411
		5.6411	5.6329	5.6263
		7.5775	7.6401	7.6991
***b*/Å**	7.5434	7.5346	7.5175	7.5000
		7.5311	7.5018	7.4757
		5.3331	5.3785	5.4243
***c*/Å**	5.3100	5.3028	5.2889	5.2750
		5.2969	5.2670	5.2414
		227.52	230.19	232.71
***V*/Å^3**	226.01	225.46	224.32	223.17
		225.03	222.56	220.45

Table II. Fitting parameters for $Gd_{1-y}R_yMn_{0.7}Co_{0.3}O_3$.

Samples R concentration y		$M_{Mn,\,Co}$/emu g^{-1}	H_{int}/kOe	Θ/K
La series	0.5	17	-1.2	-9.4
	0.3	8.3	-5.4	-19
	0.1	6.3	-5.6	-12
$GdMn_{0.7}Co_{0.3}O_3$	0.0	6.1	-7.4	-16
Y series	0.1	5.0	-5.9	-14
	0.3	3.8	-3.9	-9.9
	0.5	3.4	-4.0	-15
Lu series	0.1	4.3	-6.0	-15
	0.3	2.1	-3.6	-22
	0.5	0.38	-0.7	-36

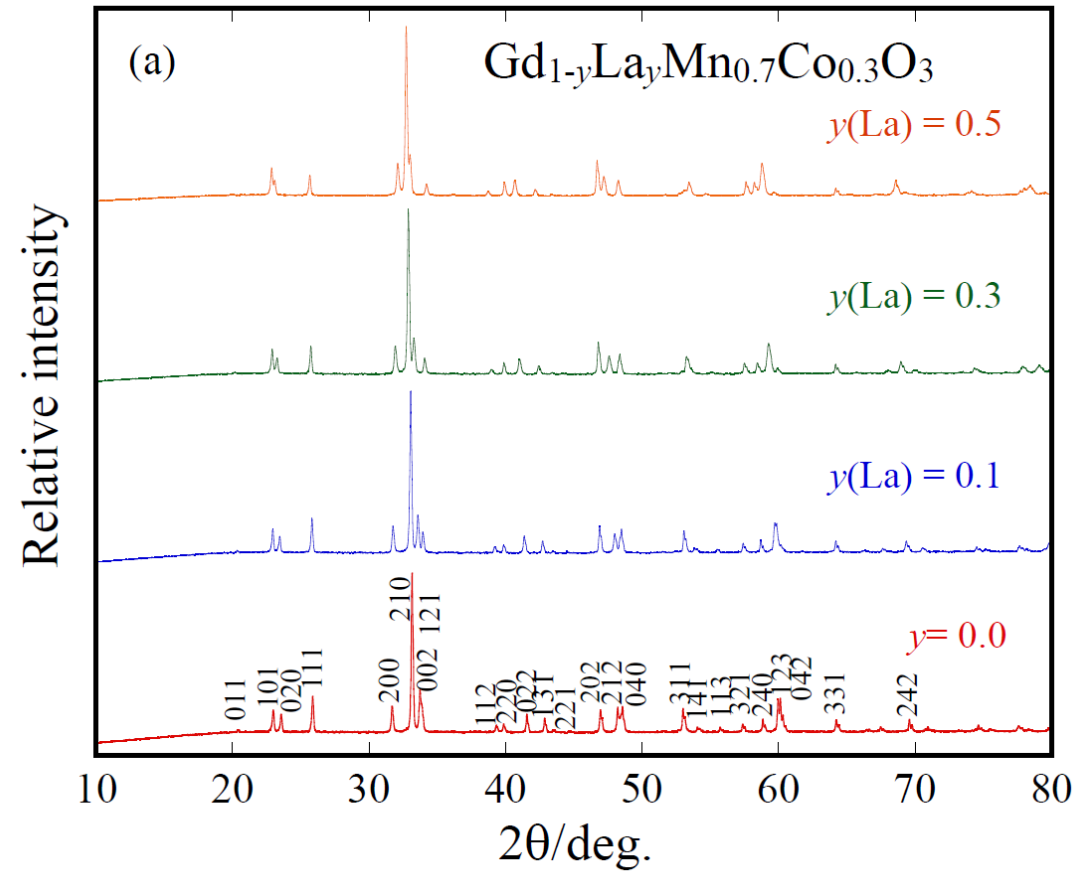
(a)
$Gd_{1-y}La_yMn_{0.7}Co_{0.3}O_3$
y(La) = 0.5
y(La) = 0.3
y(La) = 0.1
y= 0.0
Relative intensity
011
101
020
111
200
210
002
121
112
220
022
131
221
202
212
040
311
141
113
321
240
123
042
331
242
10
20
30
40
50
60
70
80
2θ/deg.

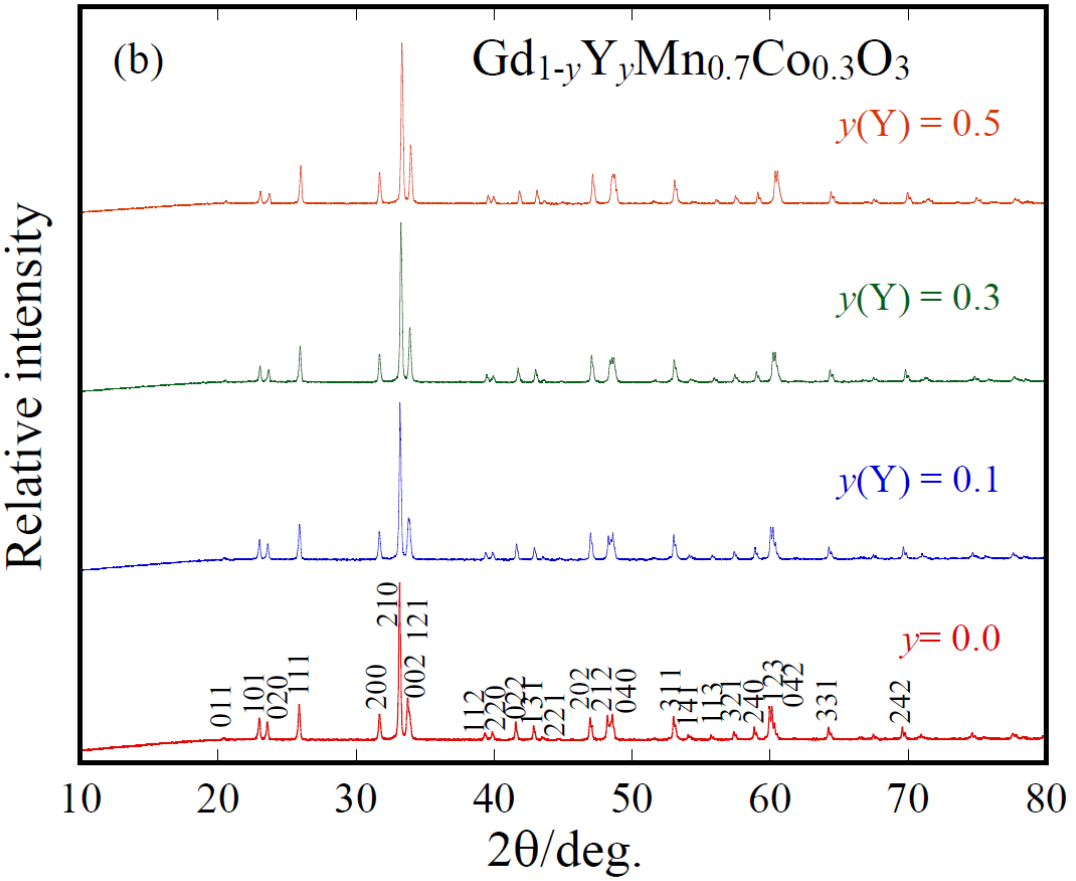
(b)
$Gd_{1-y}Y_yMn_{0.7}Co_{0.3}O_3$
y(Y) = 0.5
y(Y) = 0.3
y(Y) = 0.1
y= 0.0
Relative intensity
011
101
020
111
200
210
002
121
112
220
022
131
221
202
212
040
311
141
113
321
240
123
042
331
242
10
20
30
40
50
60
70
80
2θ/deg.

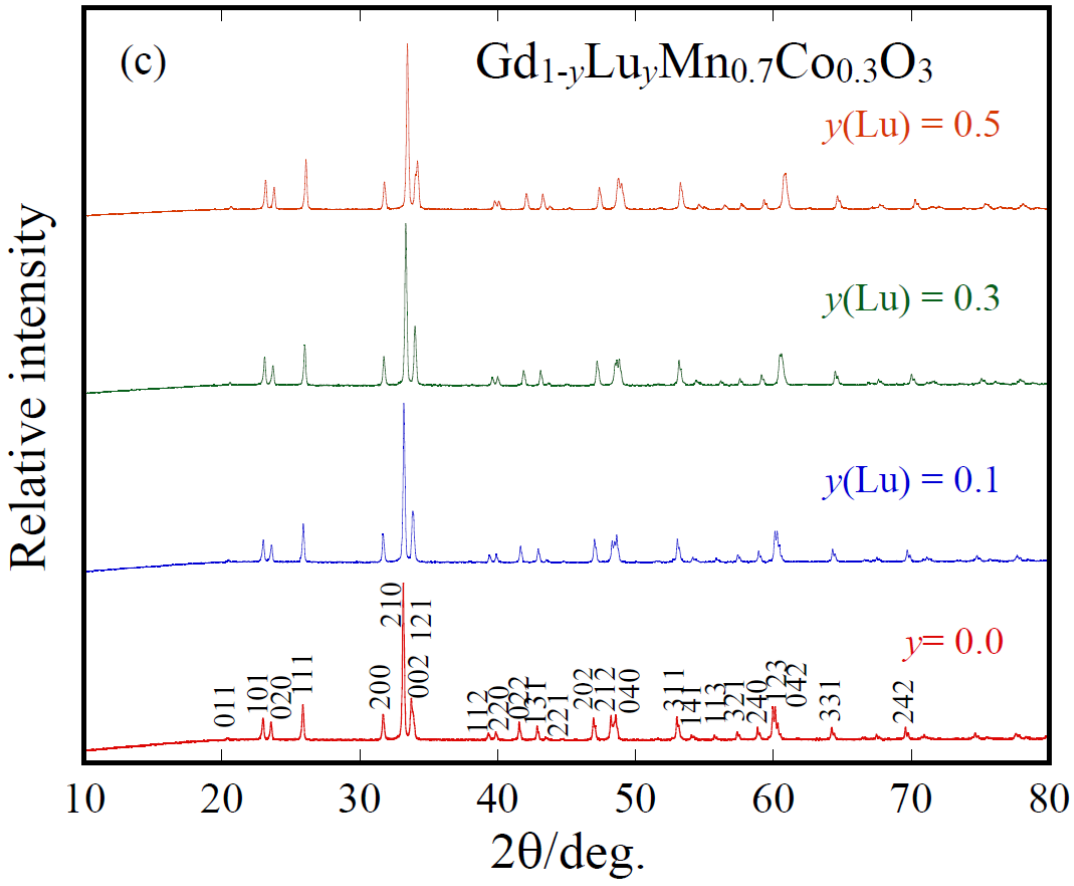

Fig. 1. XRD patterns for $Gd_{1-y}R_yMn_{0.7}Co_{0.3}O_3$ with y=0.1, 0.3 and 0.5 with substitution by the non-magnetic elements La, Y and Lu. (a), (b), and (c) correspond to $Gd_{1-y}La_yMn_{0.7}Co_{0.3}O_3$, $Gd_{1-y}Y_yMn_{0.7}Co_{0.3}O_3$, and $Gd_{1-y}Lu_yMn_{0.7}Co_{0.3}O_3$, respectively,

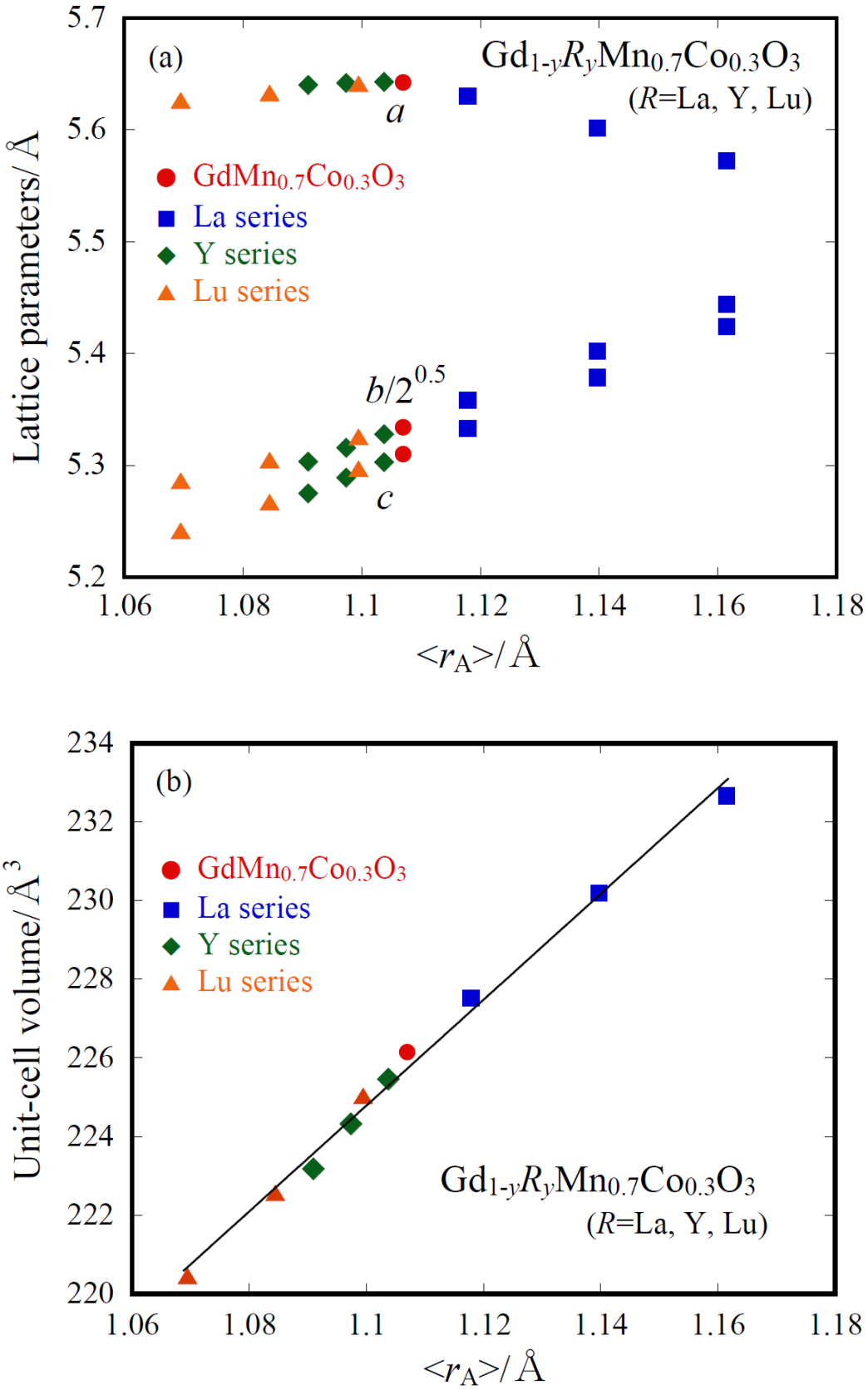

Fig. 2. Average ion radius $\langle r_A \rangle$ dependence of (a) lattice parameters a, $b/\sqrt{2}$, and c. and (b) unit-cell volume V.

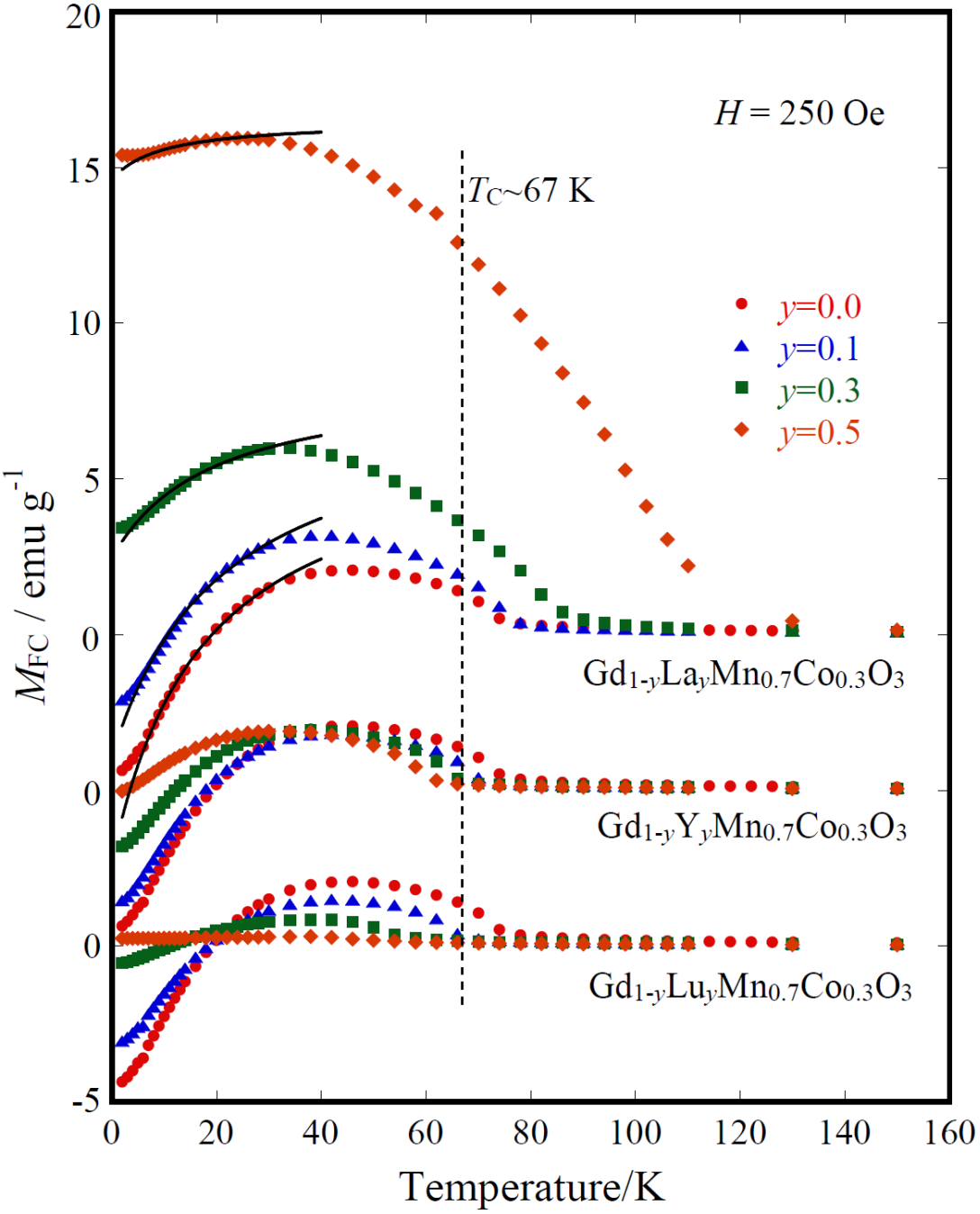

Fig. 3. Temperature dependence of M_{FC} for $Gd_{1-y}R_yMn_{0.7}Co_{0.3}O_3$. Broken line shows T_C for $GdMn_{0.7}Co_{0.3}O_3$. The solid lines in La series are fits using Eq. (4).

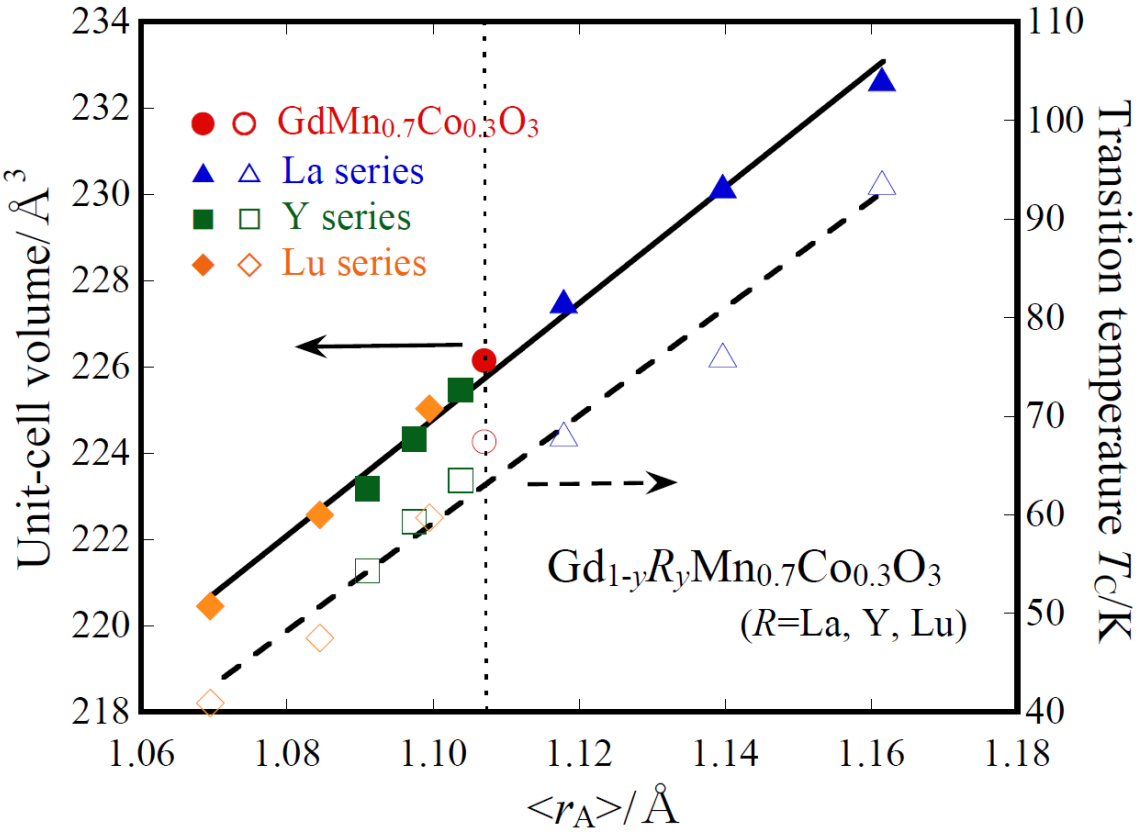

Fig. 4. V and T_C as a function of <r_A>. Their linear dependence with the same slope suggests that there is a correlation between V and T_C. The dotted line denotes the ion radius of Gd^{3+}.

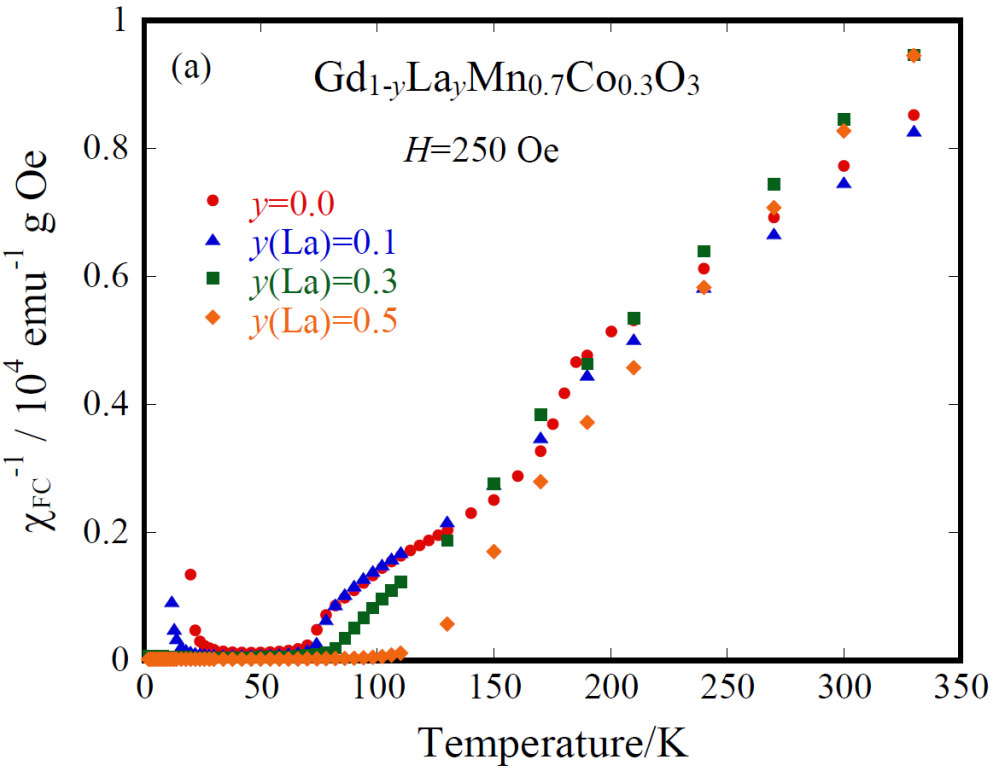
(a)
Gd1-yLayMn0.7Co0.3O3
H=250 Oe
y=0.0
y(La)=0.1
y(La)=0.3
y(La)=0.5
χFC-1 / 10^4 emu-1 g Oe
Temperature/K
0
0.2
0.4
0.6
0.8
1
0
50
100
150
200
250
300
350

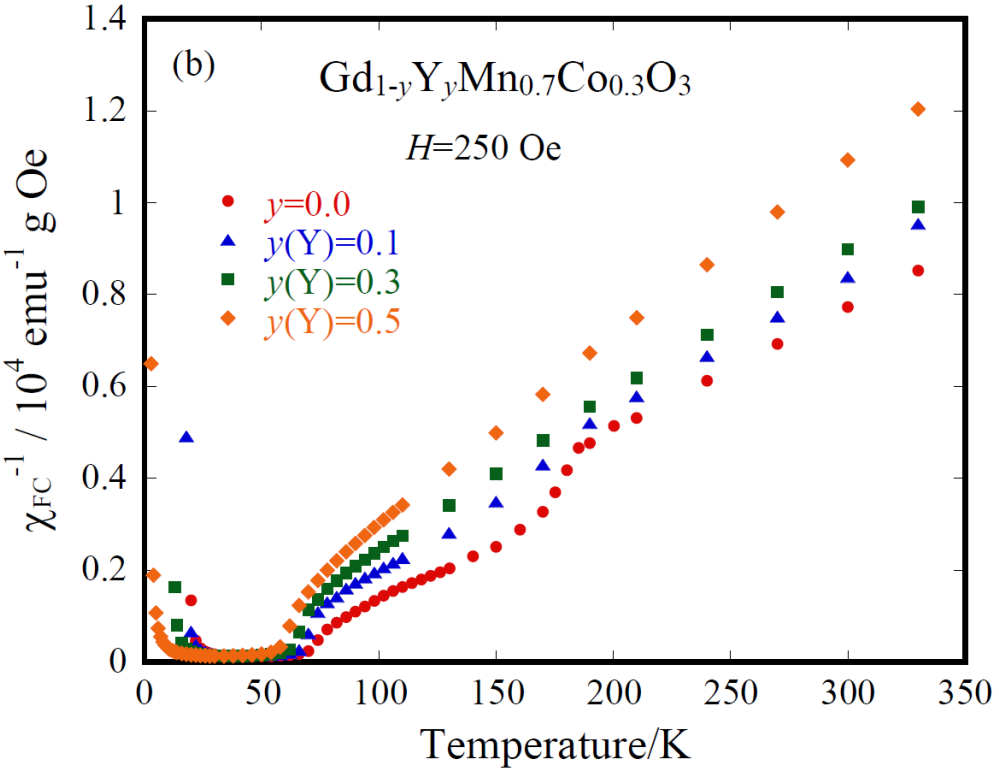
(b)
Gd1-yYyMn0.7Co0.3O3
H=250 Oe
y=0.0
y(Y)=0.1
y(Y)=0.3
y(Y)=0.5
χFC-1 / 10^4 emu-1 g Oe
Temperature/K
0
0.2
0.4
0.6
0.8
1
1.2
1.4
0
50
100
150
200
250
300
350

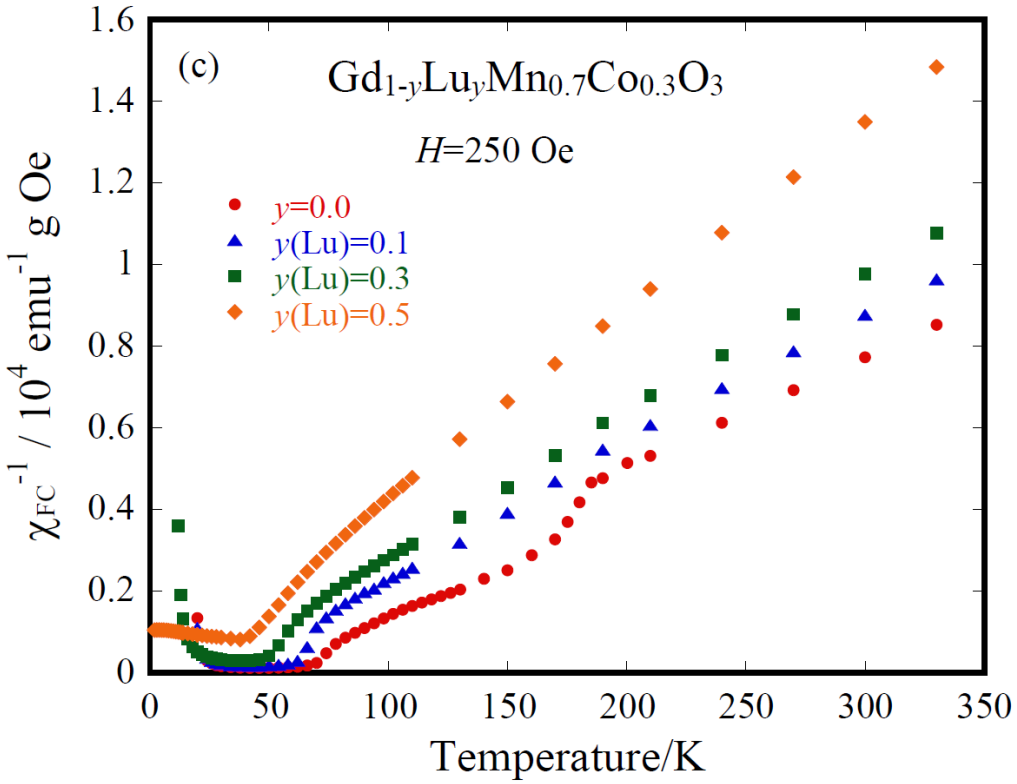

Figs. 5. Inverse magnetic susceptibility $\chi_{FC}^{-1}=H/M_{FC}$ for (a) La series, (b) Y series, and (c) for Lu series.

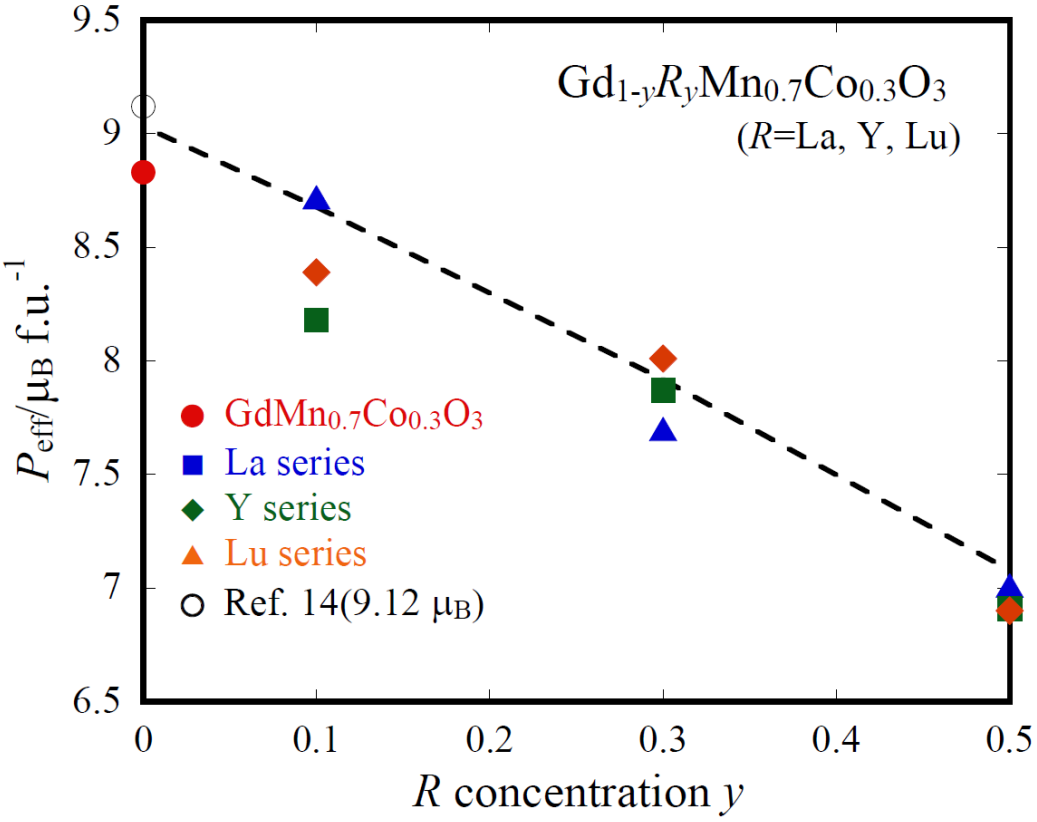

Fig. 6. R concentration dependence of effective magnetic moment P_{eff} for $Gd_{1-y}R_yMn_{0.7}Co_{0.3}O_3$ (R=La, Y, and Lu).